Chapter 21

Fundamentals of Machining

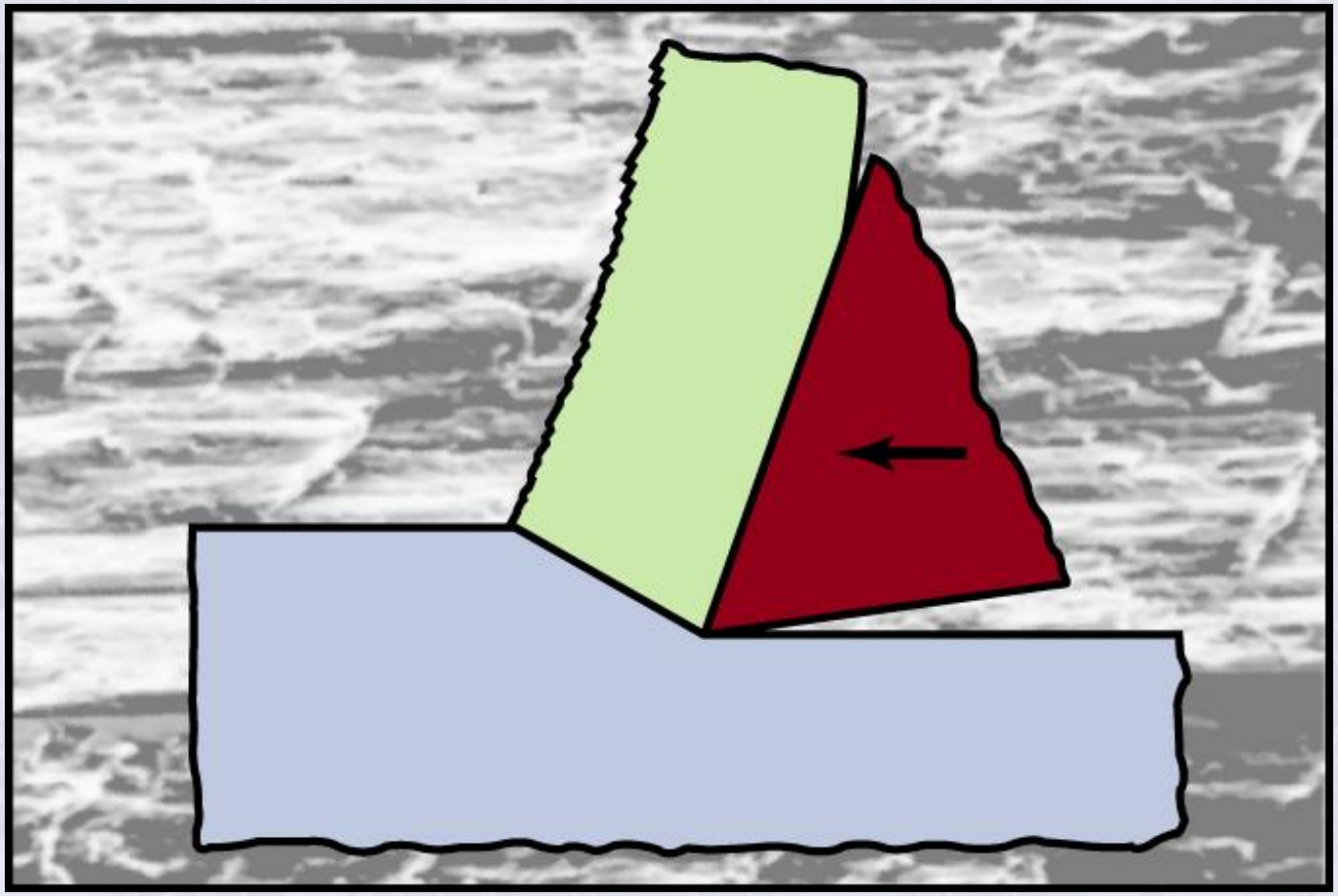

Manufacturing, Engineering & Technology, Fifth Edition, by Serope Kalpakjian and Steven R. Schmid

Common Machining Operations

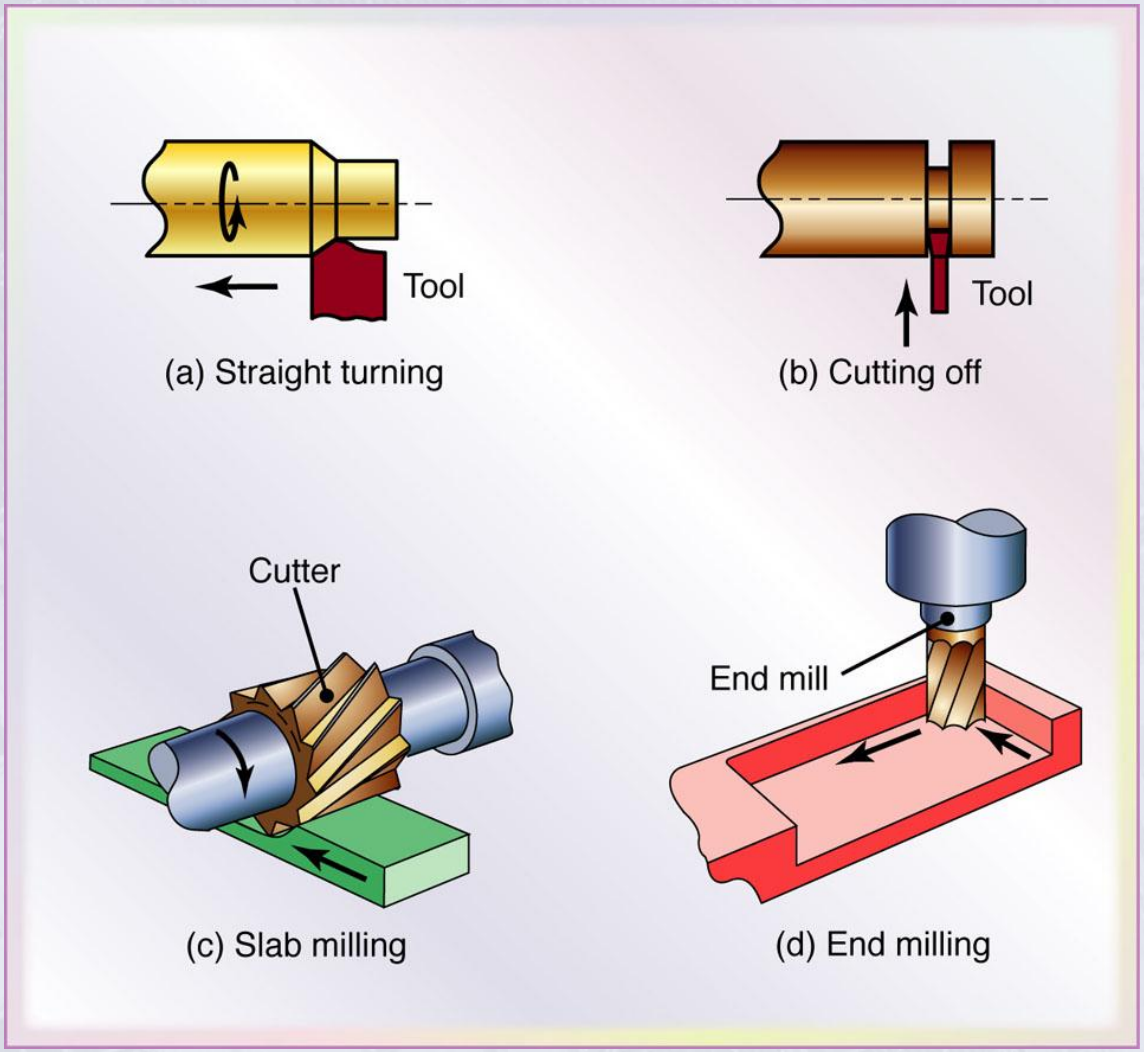

Figure 21.1 Some examples of common machining operations.

The Turning Operation

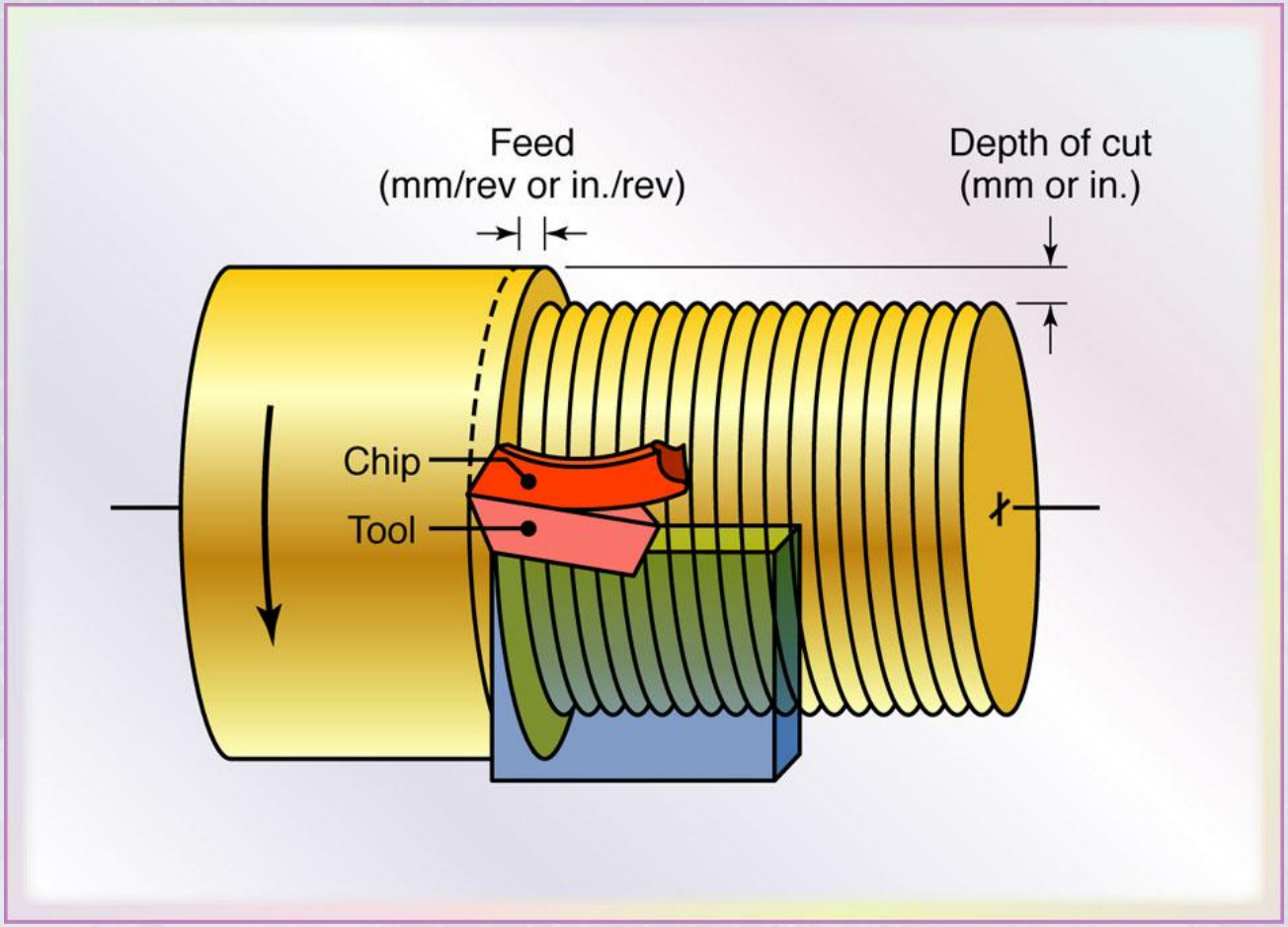

Figure 21.2 Schematic illustration of the turning operation showing various features.

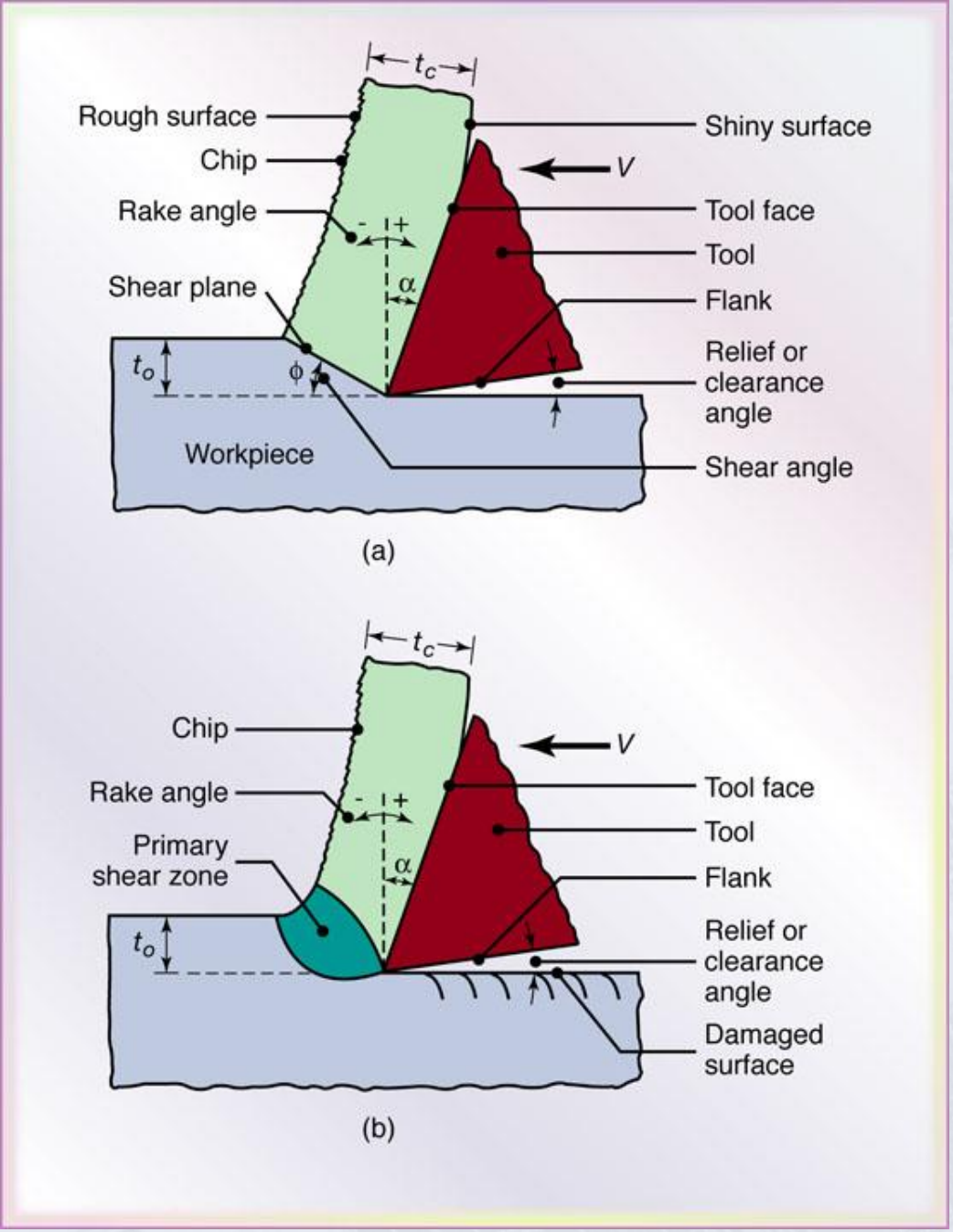

Two-Dimensional Cutting Process

Figure 21.3 Schematic illustration of a two-dimensional cutting process, also called orthogonal cutting: (a) Orthogonal cutting with a well-defined shear plane, also known as the Merchant Model. Note that the tool shape, depth of cut, t_o, and the cutting speed, V, are all independent variables, (b) Orthogonal cutting without a well-defined shear plane.

Factors Influencing Machining Operations

TABLE 21.1

Factors Influencing Machining Operations

Parameter	Influence and interrelationship
Cutting speed, depth of cut, feed, cutting fluids	Forces, power, temperature rise, tool life, type of chip, surface finish and integrity
Tool angles	As above; influence on chip flow direction; resistance to tool wear and chipping
Continuous chip	Good surface finish; steady cutting forces; undesirable, especially in automated machinery
Built-up edge chip	Poor surface finish and integrity; if thin and stable, edge can protect tool surfaces
Discontinuous chip	Desirable for ease of chip disposal; fluctuating cutting forces; can affect surface finish and cause vibration and chatter
Temperature rise	Influences tool life, particularly crater wear and dimensional accuracy of workpiece; may cause thermal damage to workpiece surface
Tool wear	Influences surface finish and integrity, dimensional accuracy, temperature rise, forces and power
Machinability	Related to tool life, surface finish, forces and power, and type of chip

Mechanics of Cutting

Cutting ratio, $r = \frac{t_o}{t_c} = \frac{\sin\phi}{\cos(\phi - \alpha)}$

Shear angle predict

$\phi = 45 + \frac{\alpha}{2} - \frac{\beta}{2}$

$\phi = 45 + \alpha - \beta$

Velocities, $V_c = \frac{V\sin\phi}{\cos(\phi - \alpha)}$

Chip Formation by Shearing

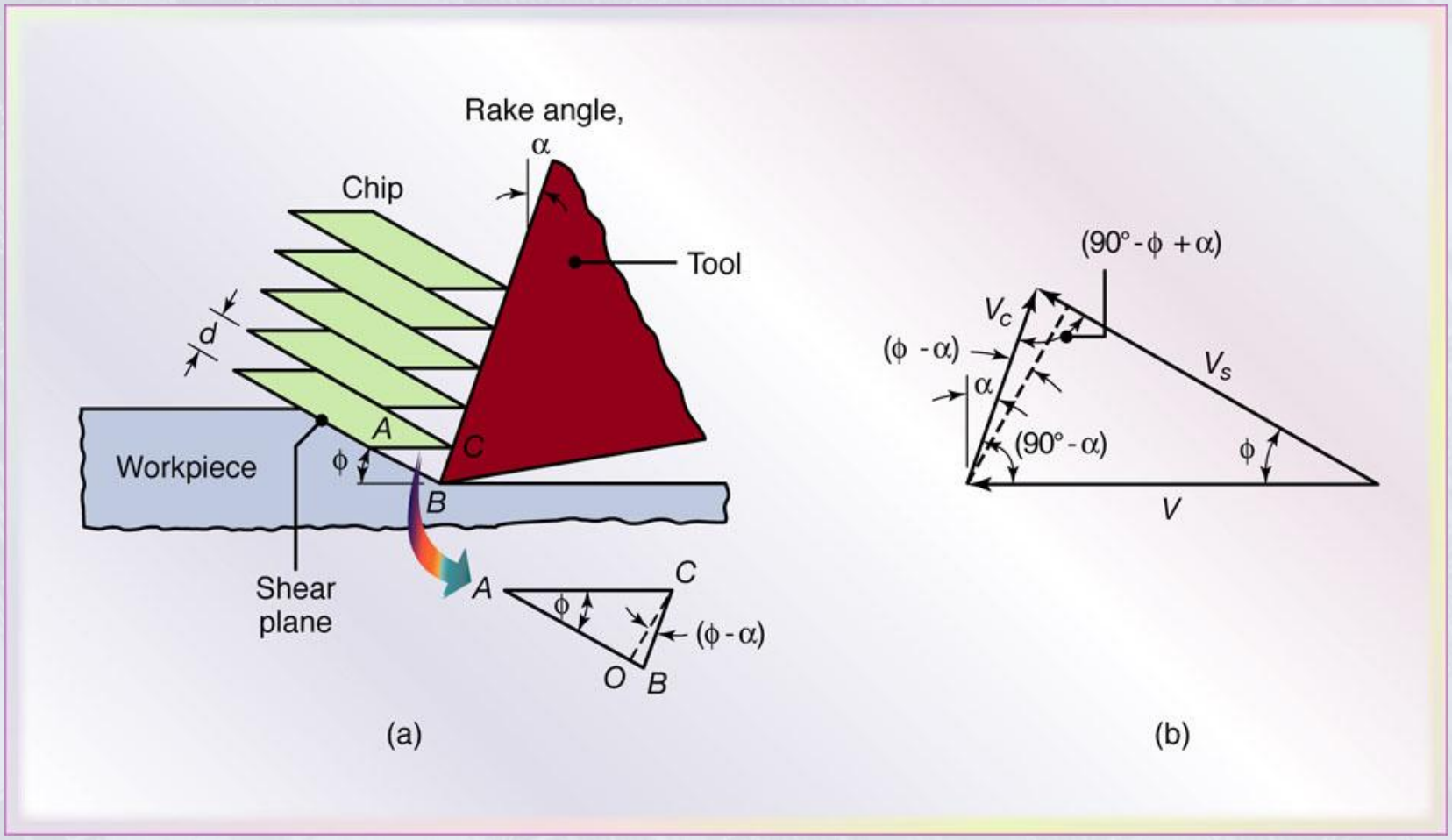

Figure 21.4 (a) Schematic illustration of the basic mechanism of chip formation by shearing. (b) Velocity diagram showing angular relationships among the three speeds in the cutting zone.

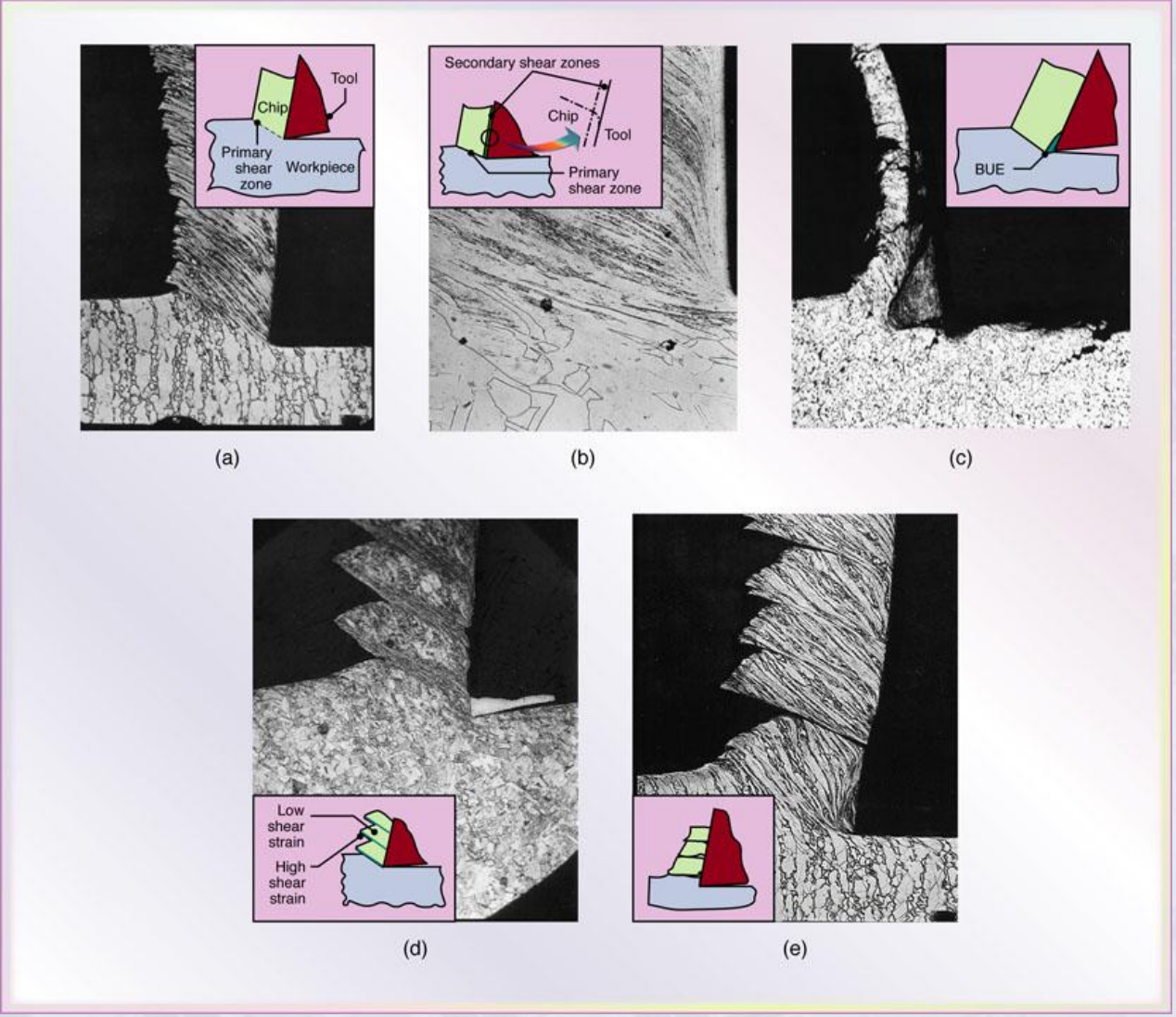

Chips Produced in Orthogonal Metal Cutting

Figure 21.5 Basic types of chips produced in orthogonal metal cutting, their schematic representation, and photomicrographs of the cutting zone: (a) continuous chip with narrow, straight, and primary shear zone; (b) continuous chip with secondary shear zone at the cip-tool interface; (c) built-up edge; (d) segmented or nonhomogeneous chip; and (e) discontinuous chip. *Source*: After M.C. Shaw, P.K. Wright, and S. Kalpakjian.

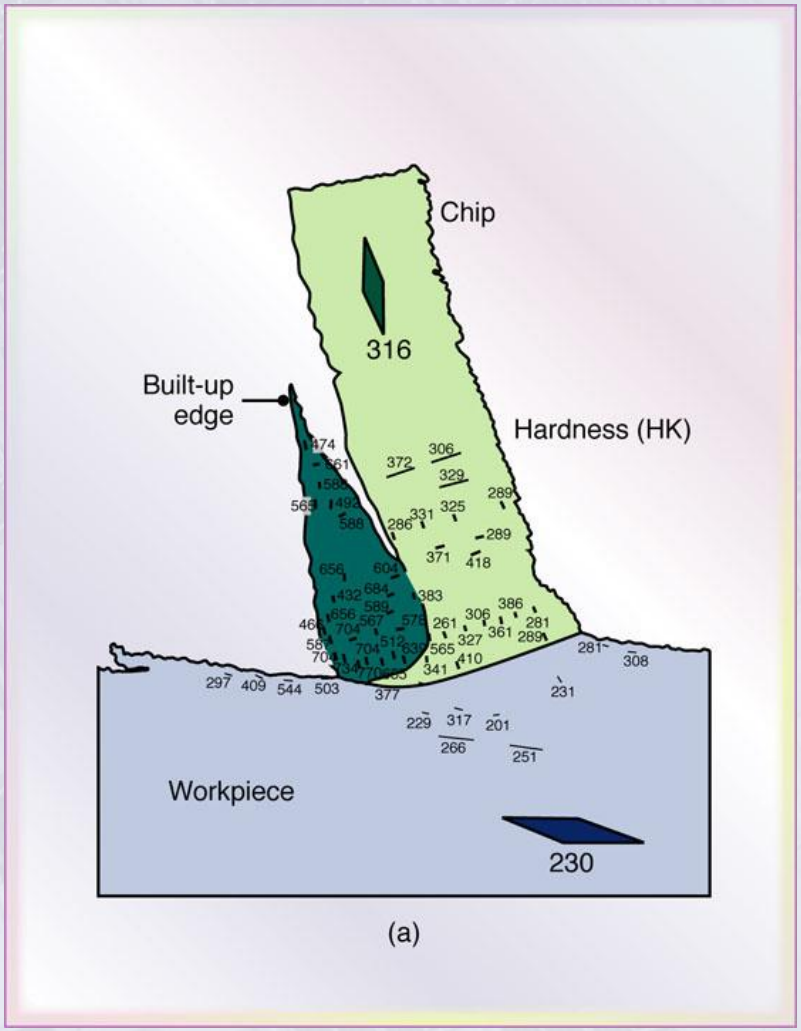

Built-up Edge

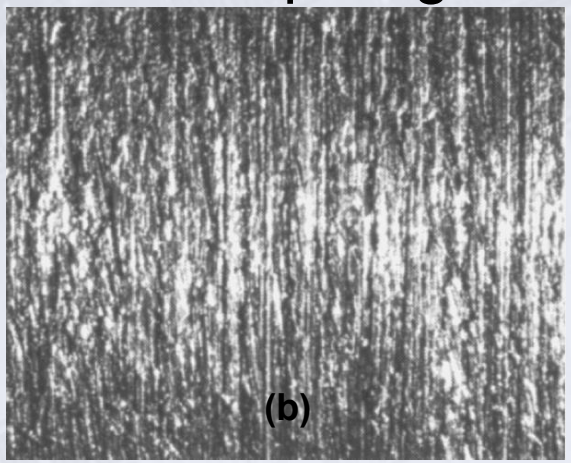

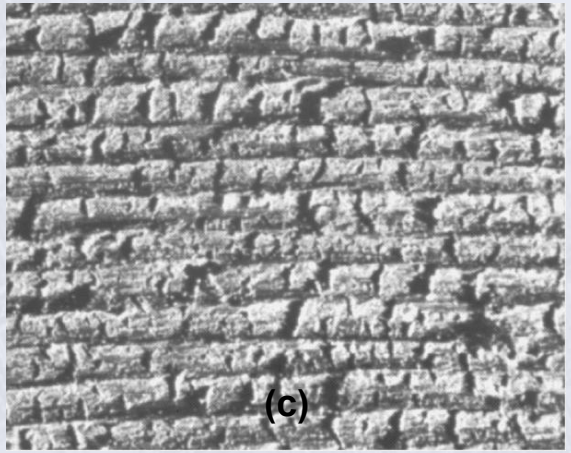

Figure 21.6 (a) Hardness distribution with a built-up edge in the cutting zone (material, 3115 steel). Note that some regions in the built-up edge are as much as three times harder than the bulk metal of the workpiece. (b) Surface finish produced in turning 5130 steel with a built-up edge. (c) Surface finish on 1018 steel in face milling. Magnifications: 15x. *Source*: Courtesy of Metcut Research Associates, Inc.

Manufacturing, Engineering & Technology, Fifth Edition, by Serope Kalpakjian and Steven R. Schmid

Chip Breaker

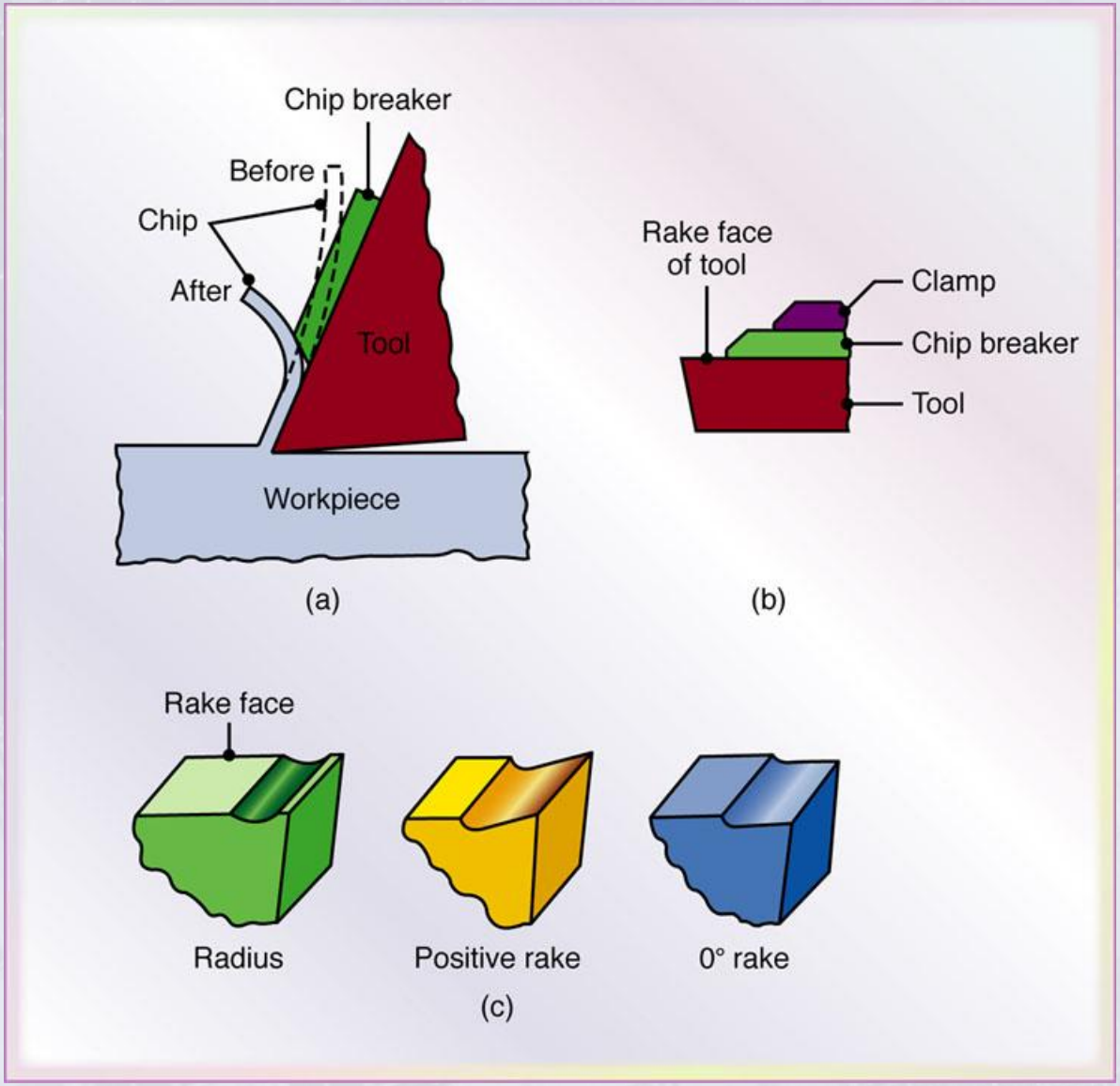

Figure 21.7 (a) Schematic illustration of the action of a chip breaker. Note that the chip breaker decreases the radius of curvature of the chip and eventually breaks it. (b) Chip breaker clamped on the rake face of a cutting tool. (c) Grooves in cutting tools acting as chip breakers. Most cutting toold used now are *inserts* with built-in chip breaker features.

Chips Produced in Turning

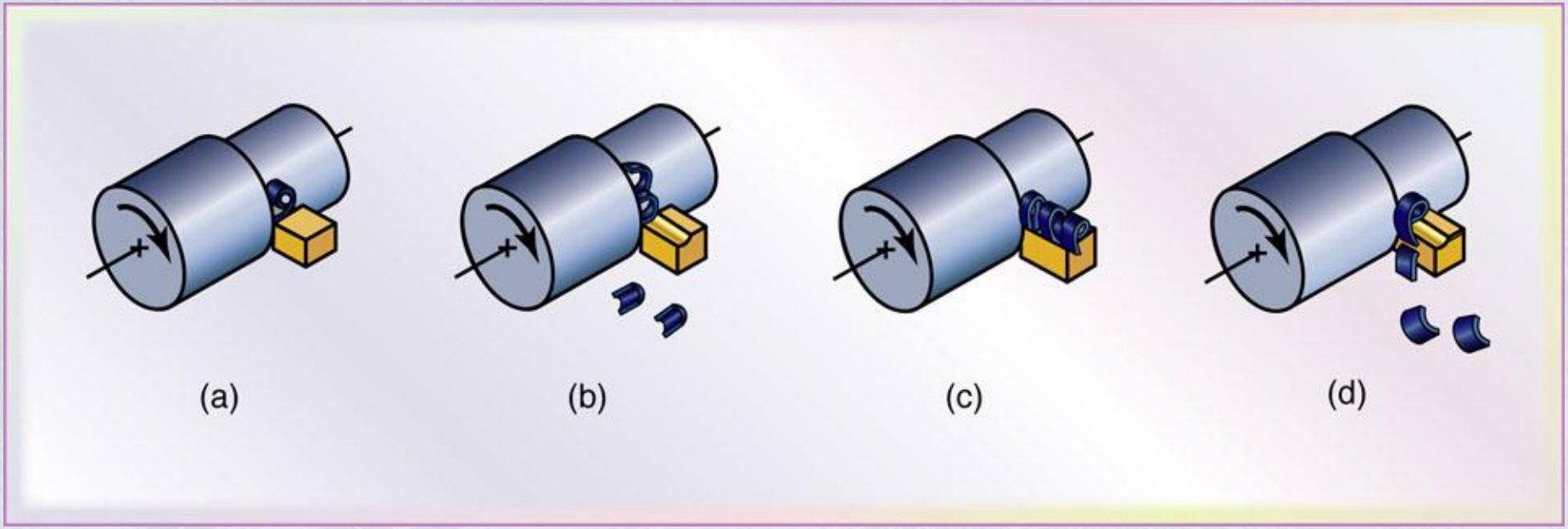

Figure 21.8 Chips produced in turning: (a) tightly curled chip; (b) chip hits workpiece and breaks; (c) continuous chip moving radially away from workpiece; and (d) chip hits tool shank and breaks off. *Source:* After G. Boothroyd.

Cutting with an Oblique Tool

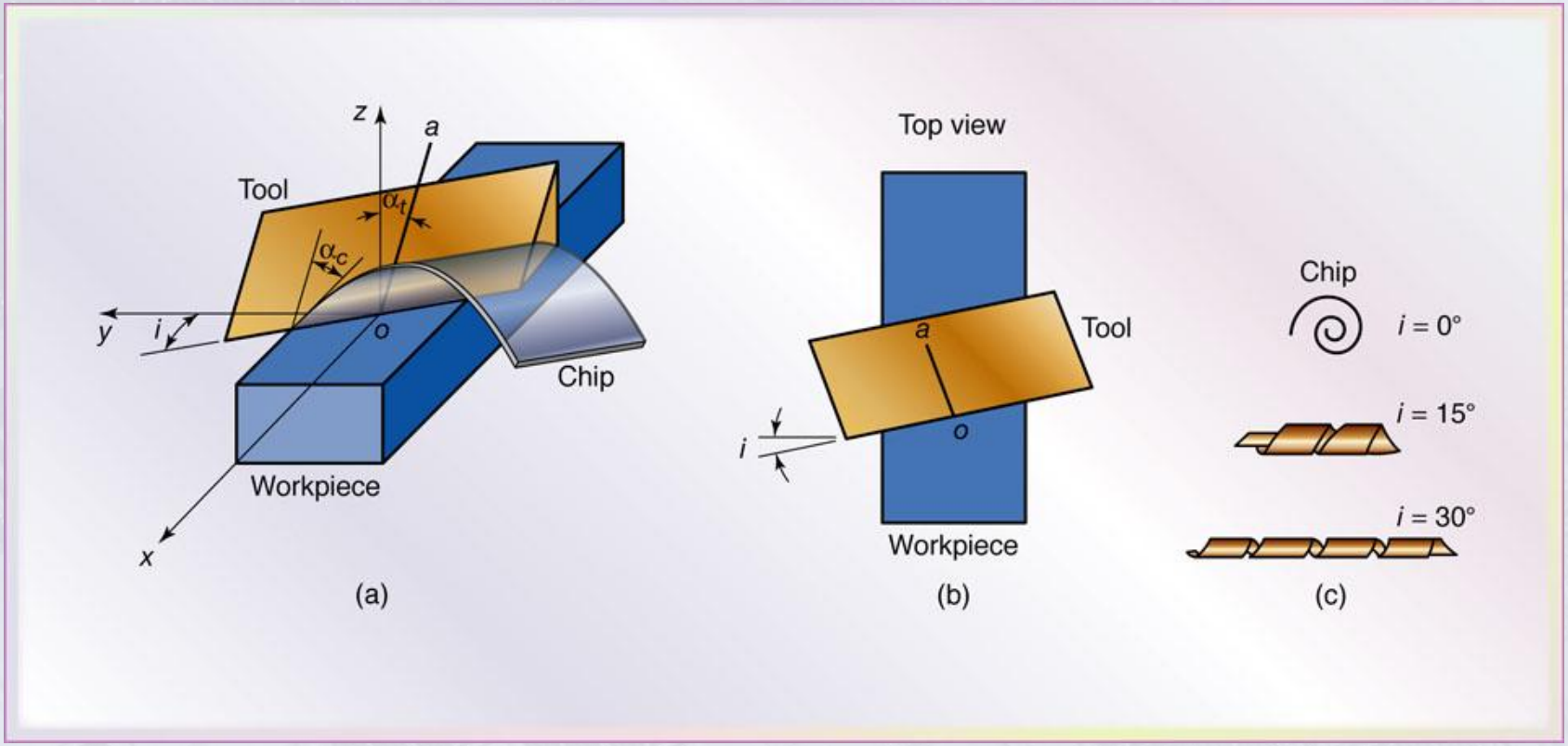

Figure 21.9 (a) Schematic illustration of cutting with an oblique tool. Note the direction of chip movement. (b) Top view, showing the inclination angle, *i*,. (c) Types of chips produced with tools at increasing inclination angles.

Right-hand Cutting Tool and Insert

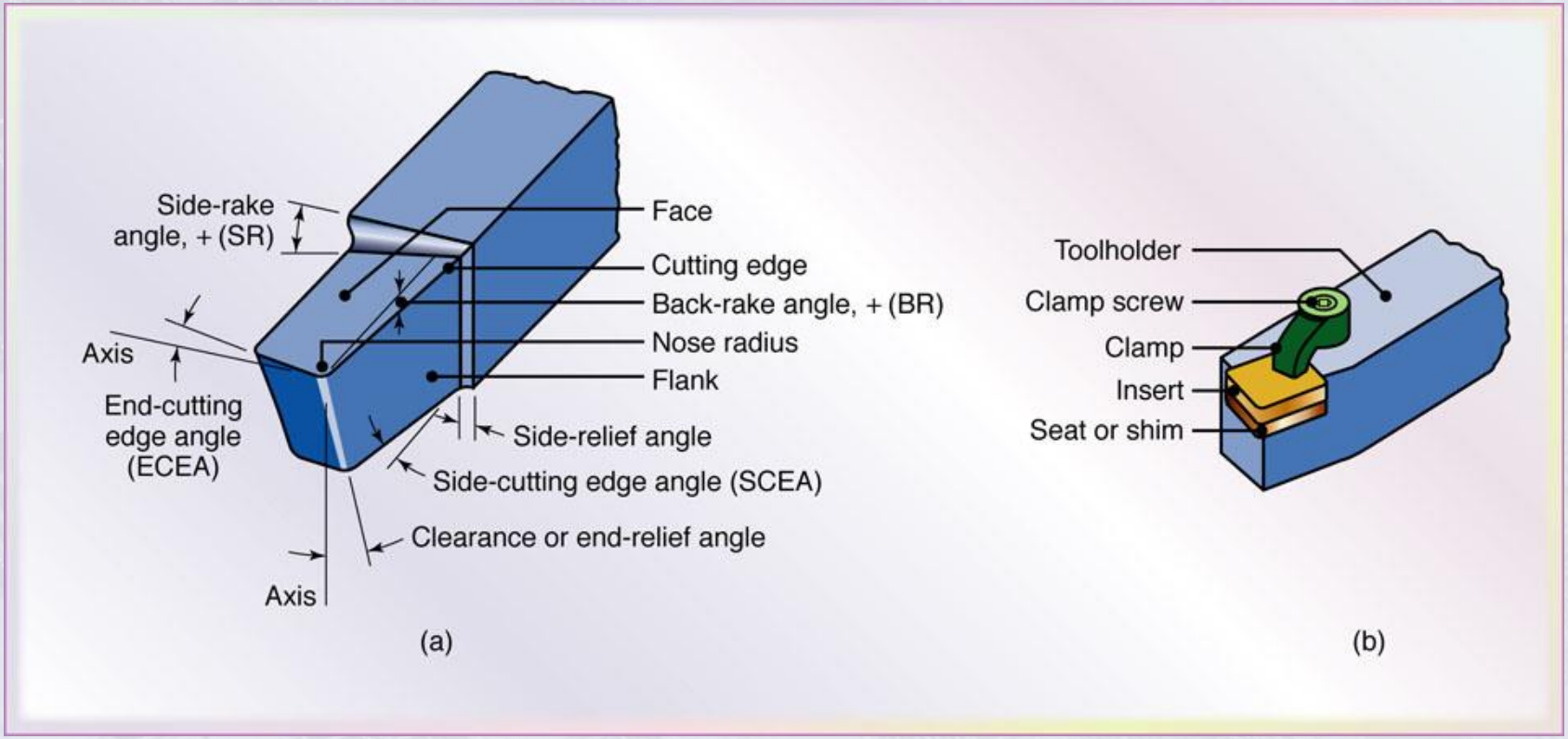

Figure 21.20 (a) Schematic illustration of right-hand cutting tool. The various angles on these tools and their effects on machining are described in Section 23.3.1 Although these tools traditionally have been produced from solid tool-steel bars, they have been replaced largely with (b) inserts made of carbides and other materials of various shapes and sizes.

Cutting Forces

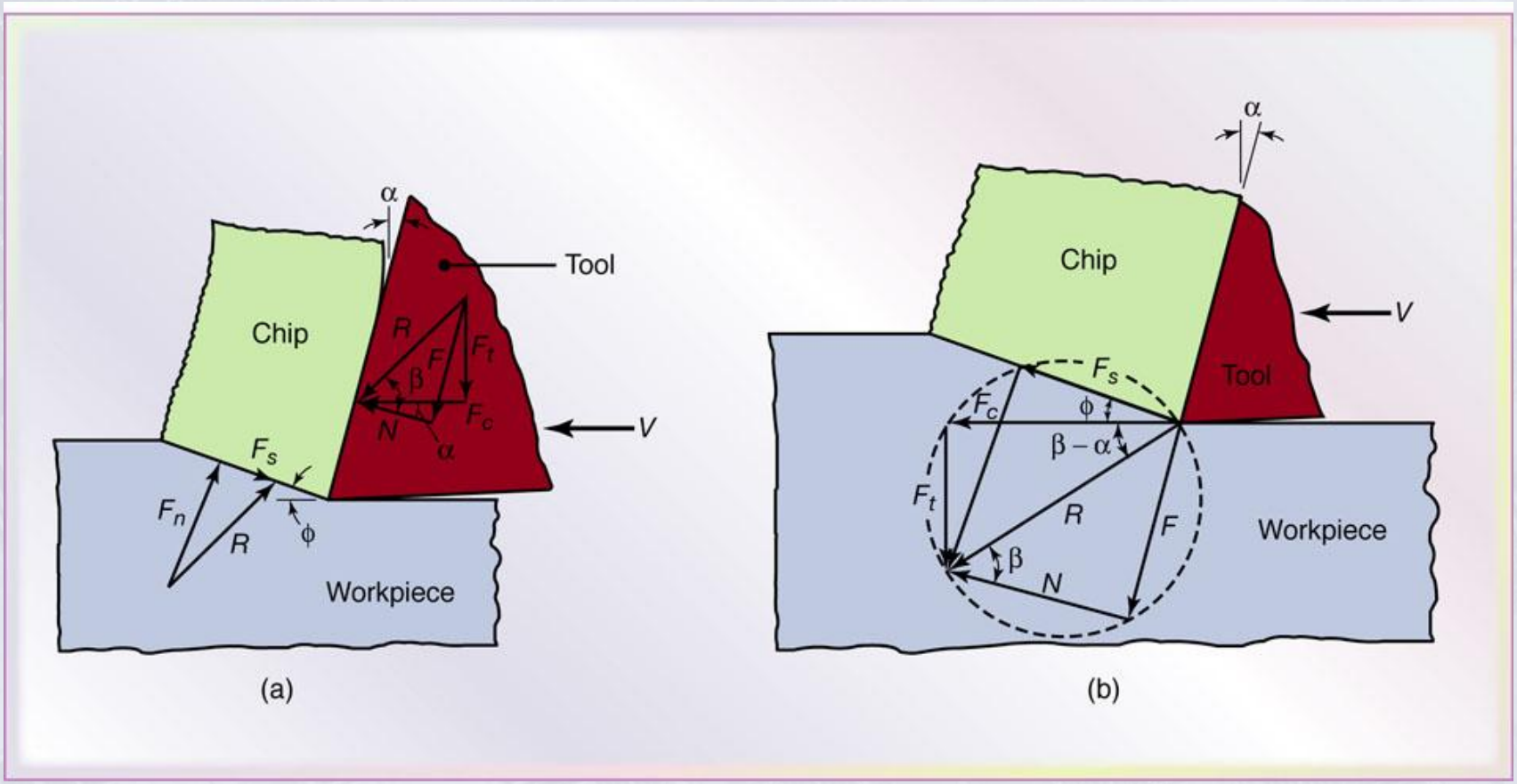

Figure 21.11 (a) Forces acting on a cutting tool during two-dimensional cutting. Note that the resultant force, *R*, must be collinear to balance the forces. (b) Force circle to determine various forces acting in the cutting zone.

Manufacturing, Engineering & Technology, Fifth Edition, by Serope Kalpakjian and Steven R. Schmid

Cutting Forces and Power

Shear force $F_s = F_c \cos\alpha - F_t \sin\alpha$

Normal force $F_n = F_c \sin\alpha + F_t \cos\alpha$

Coefficient of friction, $\mu = \frac{F}{N} = \frac{F_t + F_c \tan\alpha}{F_c - F_t \tan\alpha}$

Power $= F_c V$

Range of Energy Requirements in Cutting Operations

TABLE 21.2

Approximate Range of Energy Requirements in Cutting Operations at the Drive Motor of the Machine Tool (For Dull Tools, Multiply by 1.25)

Material	Specific energy	
	W-s/mm^3	hp-min/in^3
Aluminum alloys	0.4-1	0.15-0.4
Cast irons	1.1-5.4	0.4-2
Copper alloys	1.4-3.2	0.5-1.2
High-temperature alloys	3.2-8	1.2-3
Magnesium alloys	0.3-0.6	0.1-0.2
Nickel alloys	4.8-6.7	1.8-2.5
Refractory alloys	3-9	1.1-3.5
Stainless steels	2-5	0.8-1.9
Steels	2-9	0.7-3.4
Titanium alloys	2-5	0.7-2

Manufacturing, Engineering & Technology, Fifth Edition, by Serope Kalpakjian and Steven R. Schmid

Temperatures in Cutting Zone

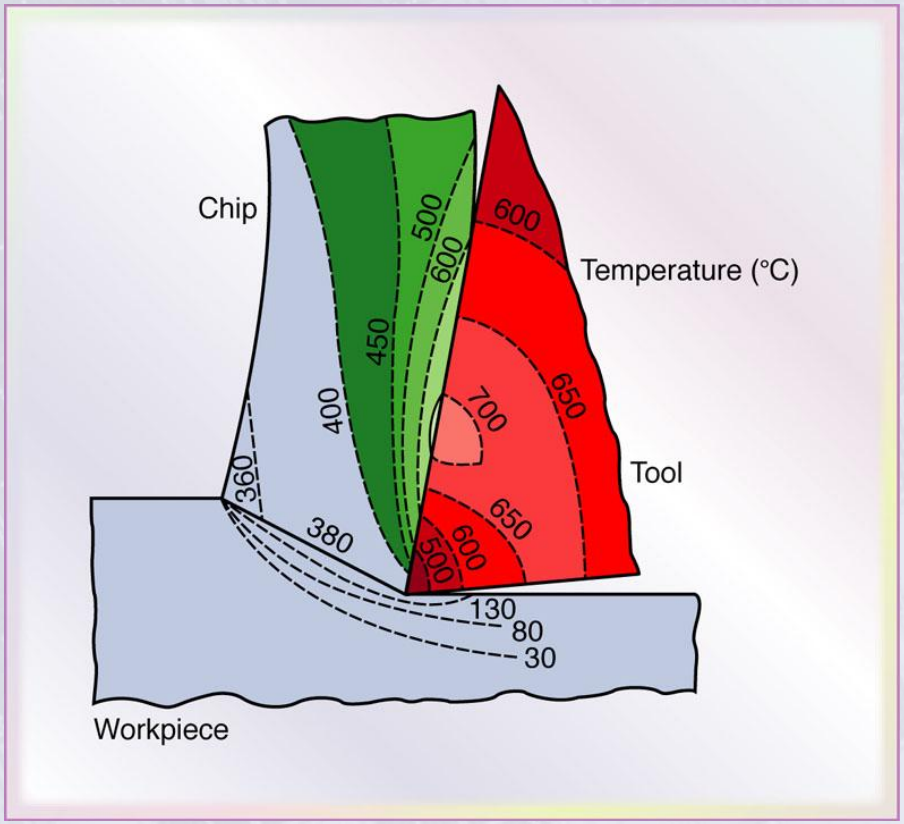

Figure 21.12 Typical temperature distribution in the cutting zone. Note the severe temperature gradients within the tool and the chip, and that the workpiece is relatively cool. *Source*: After G. Vieregge.

Mean temperature in cutting:

$$T_{mean} = \frac{1.2 Y_f}{\left(\frac{V t_o}{K}\right)^{1/3} C}$$

where

Y_f = flow stress, psi

C = volumetric specific heat, Btu/in^3-°F

K = thermal diffusivity

Temperatures Developed in Turning 52100 Steel

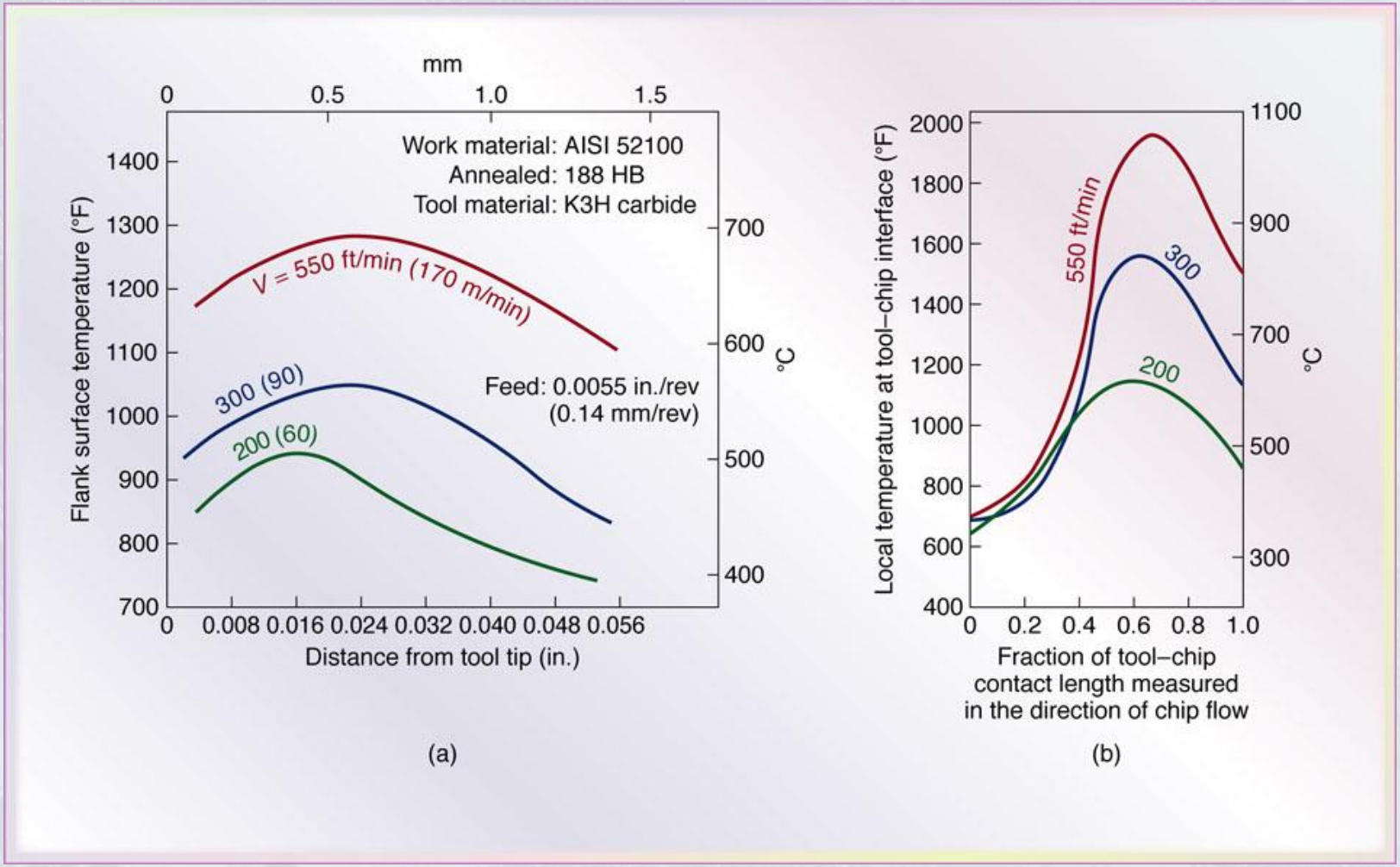

Figure 21.13 Temperatures developed in turning 52100 steel: (a) flank temperature distribution and (b) tool-ship interface temperature distribution. *Source*: After B. T. Chao and K. J. Trigger.

Manufacturing, Engineering & Technology, Fifth Edition, by Serope Kalpakjian and Steven R. Schmid

Proportion of Heat from Cutting Transferred as a Function of Cutting Speed

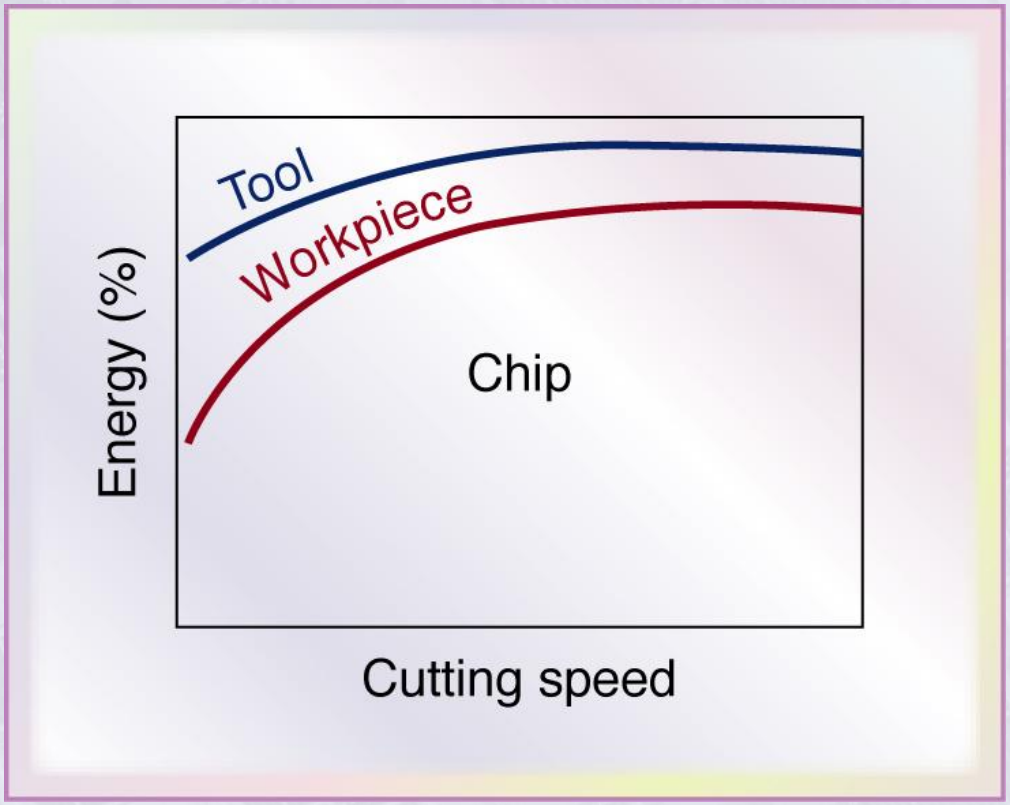

Figure 21.14 Proportion of the heat generated in cutting transferred into the tool, workpiece, and chip as a function of the cutting speed. Note that the chip removes most of the heat.

Wear Patterns on Tools

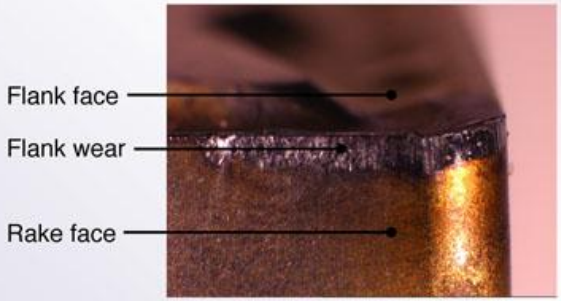

(a)

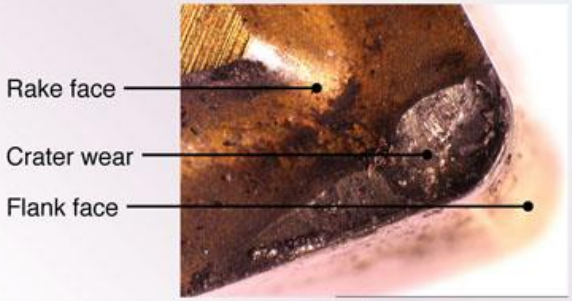

(b)

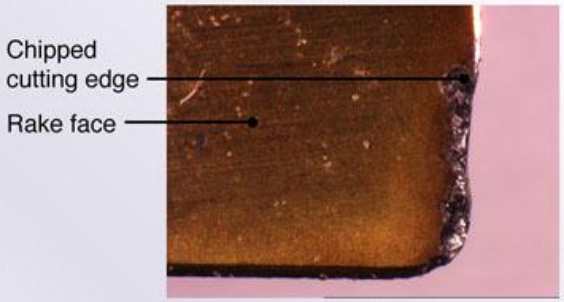

(c)

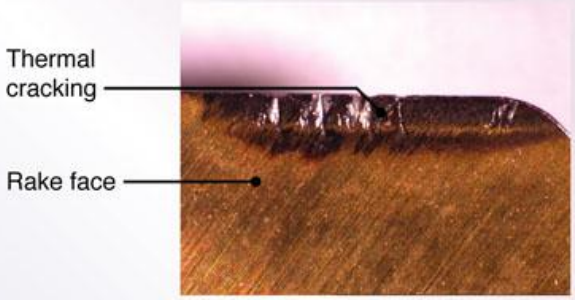

(d)

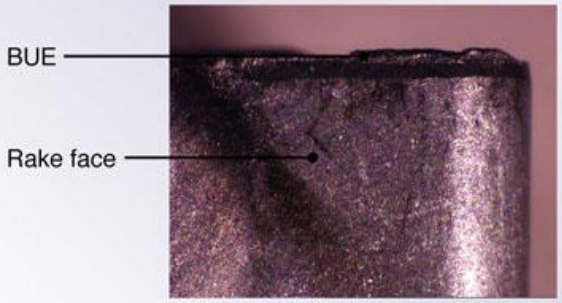

(e)

(f)

Figure 21.15 (a) Flank wear and crater wear in a cutting tool; the tool moves to the left as in Fig. 21.3. (b) View of the rake face of a turning tool, showing various wear patterns. (c) View of the flank face of a turning tool, showing various wear patterns. (d) Types of wear on a turning tool: 1. flank wear; 2. crater wear; 3. chipped cutting edge; 4. thermal cracking on rake face; 5. built-up edge; 6. catastrophic failure. (See also Fig. 21.18.) *Source*: Courtesy of Kennametal, Inc.

Taylor Tool Lofe Equation

TABLE 21.3

Ranges of *n* Values for the Taylor Eq. (21.20a) for Various Tool Materials

High-speed steels	0.08-0.2
Cast alloys	0.1-0.15
Carbides	0.2-0.5
Coated carbides	0.4-0.6
Ceramics	0.5-0.7

Taylor Equation:

$$VT^n = C$$

$$VT^n d^x f^y = C$$

Effect of Workpiece Hardness and Microstructure on Tool Life

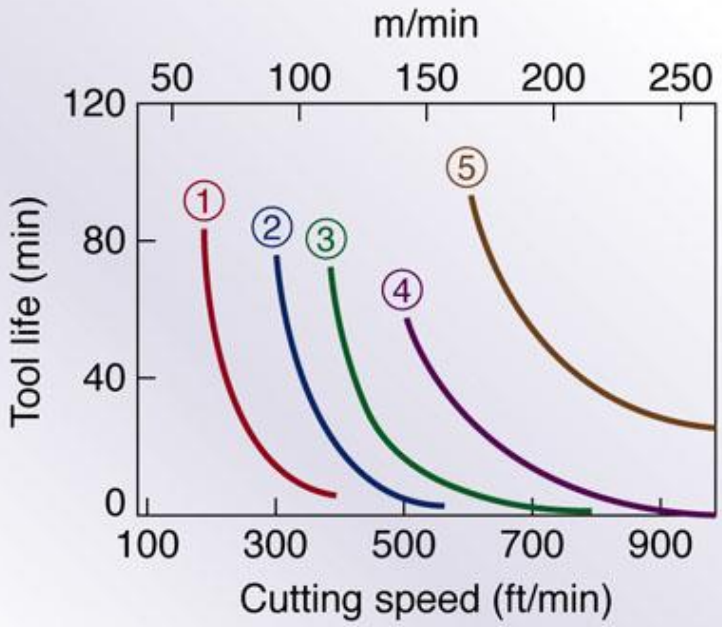

	Hardness (HB)	Ferrite	Pearlite
① As cast	265	20%	80%
② As cast	215	40	60
③ As cast	207	60	40
④ Annealed	183	97	3
⑤ Annealed	170	100	—

Figure 21.16 Effect of workpiece hardness and microstructure on tool life in turning ductile cast iron. Note the rapid decrease in tool life (approaching zero) as the cutting speed increases. Tool materials have been developed that resist high temperatures, such as carbides, ceramics, and cubic boron nitride, as will be described in Chapter 22.

Tool-life Curves

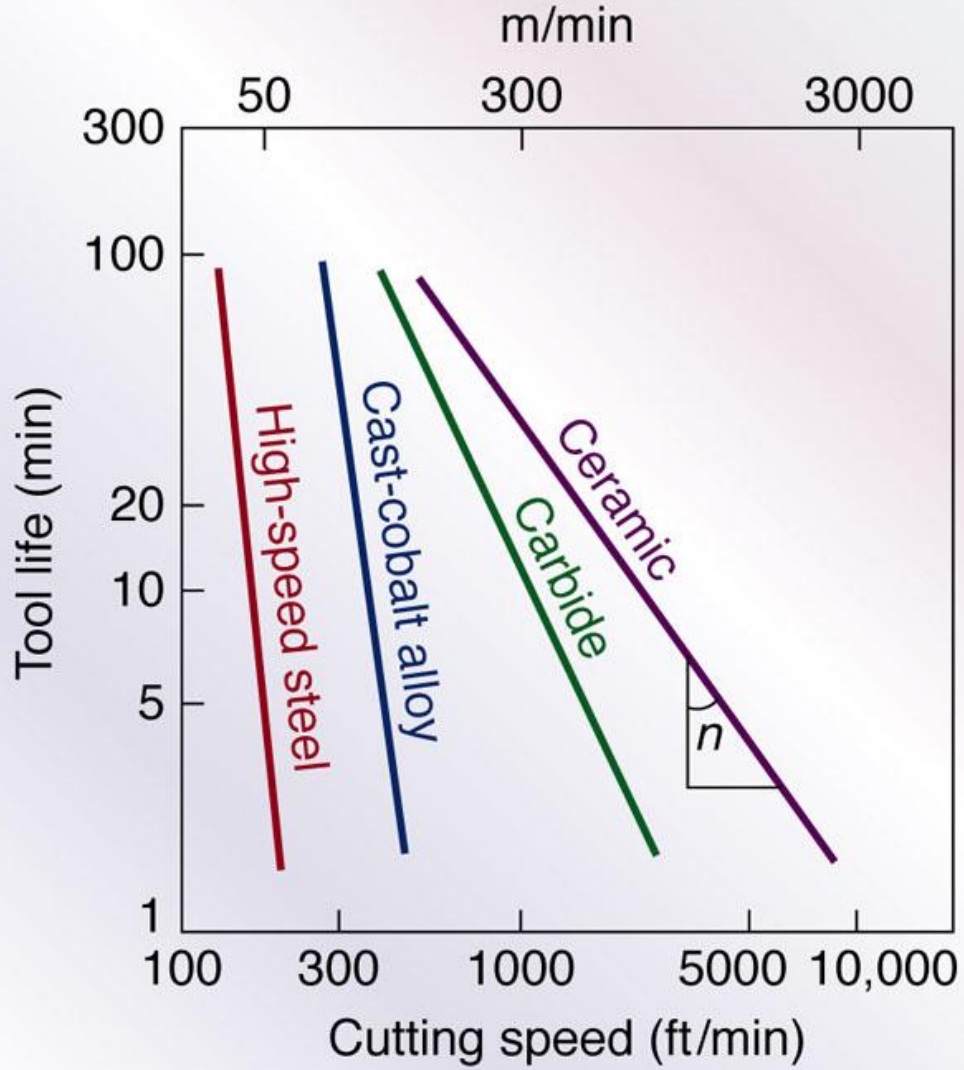

Figure 21.17 Tool-life curves for a variety of cutting-tool materials. The negative inverse of the slope of these curves is the exponent *n* in the Taylor tool-life equation and *C* is the cutting speed at *T* = 1 min, ranging from about 200 to 10,000 ft./min in this figure.

Allowable Average Wear Land for Cutting Tools

TABLE 21.4

Allowable Average Wear Land (see *VB* in Fig. 21.15c) for Cutting Tools in Various Machining Operations

Operation	Allowable wear land (mm)	
	High-speed-steel tools	Carbide tools
Turning	1.5	0.4
Face milling	1.5	0.4
End milling	0.3	0.3
Drilling	0.4	0.4
Reaming	0.15	0.15

Note: Allowable wear for ceramic tools is about 50% higher. Allowable notch wear, VB_{max}, is about twice that for *VB*.

Types of Wear seen in Cutting Tools

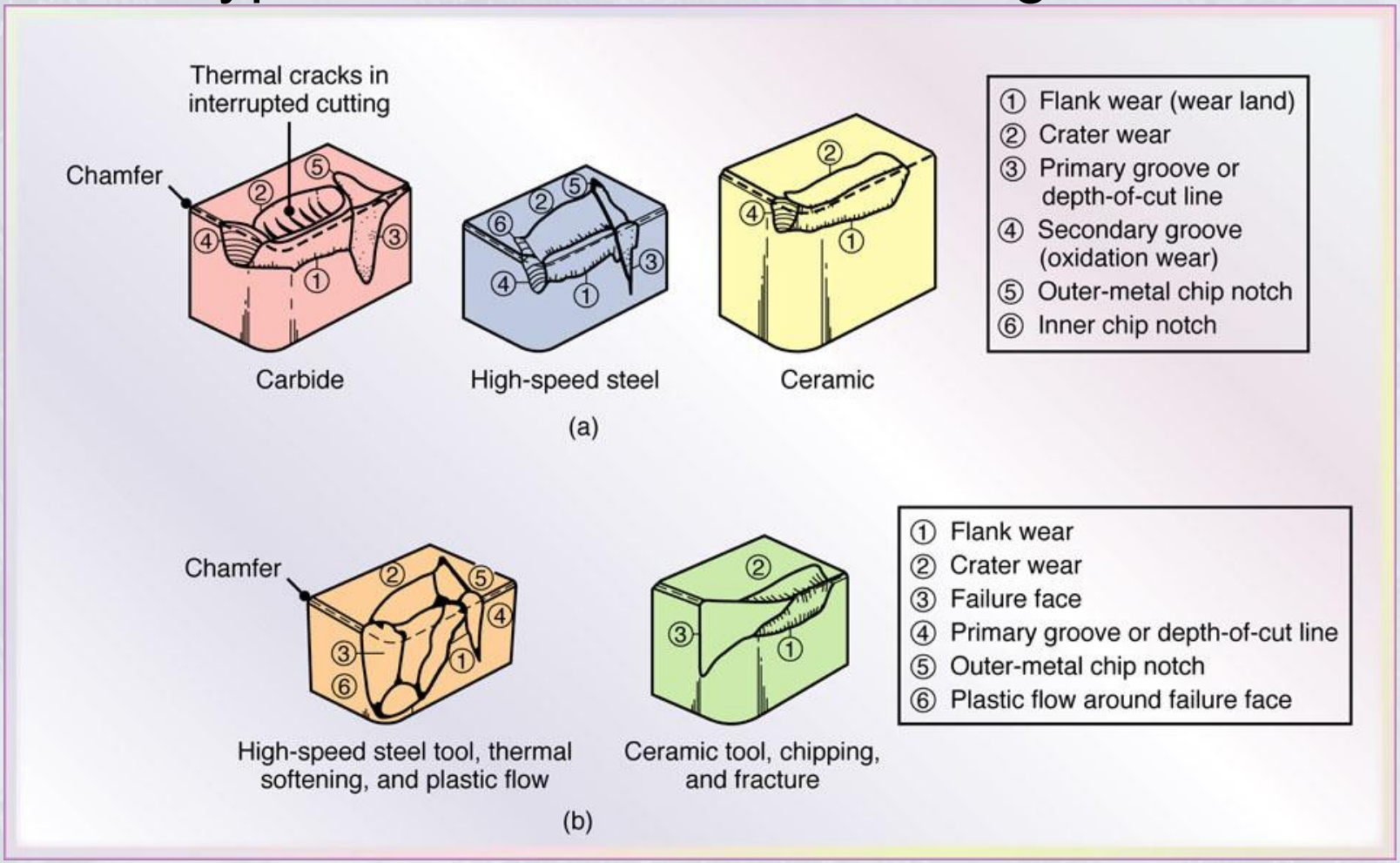

Figure 21.28 (a) Schematic illustration of types of wear observed on various cutting tools. (b) Schematic illustrations of catastrophic tool failures. A wide range of parameters influence these wear and failure patterns. *Source*: Courtesy of V. C. Venkatesh.

Manufacturing, Engineering & Technology, Fifth Edition, by Serope Kalpakjian and Steven R. Schmid

Relationship between Crater-Wear Rate and Average Tool-Chip Interface Temperature

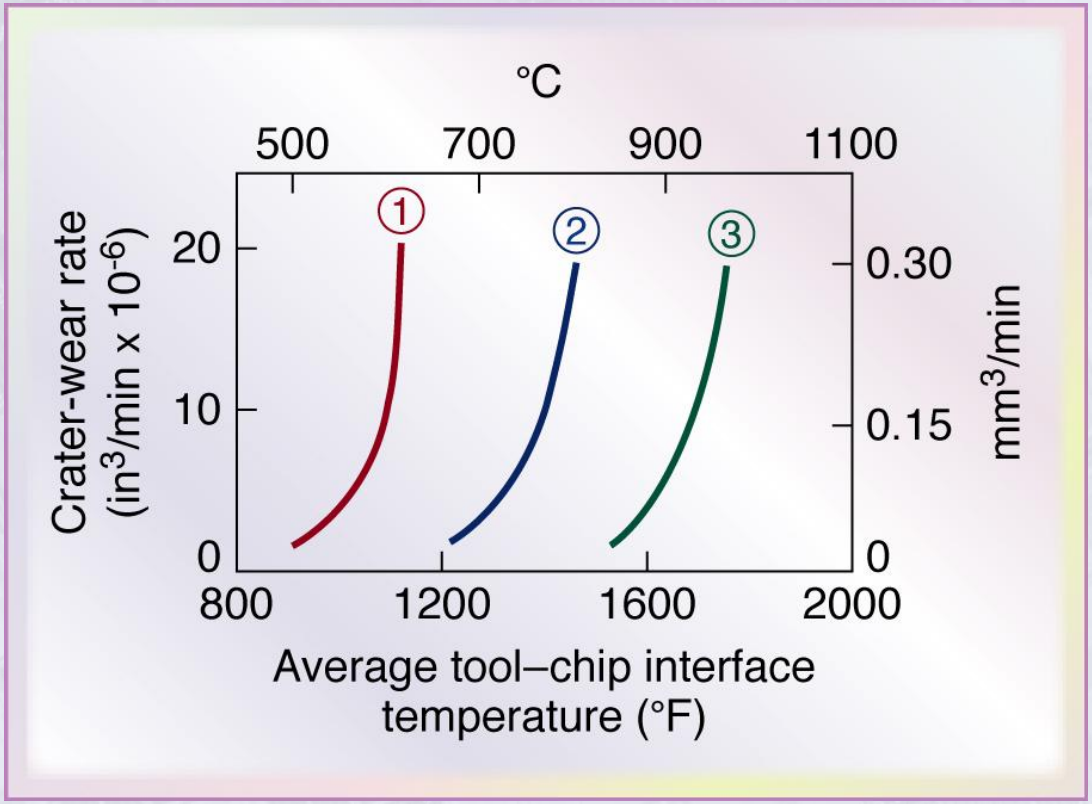

Figure 21.19 Relationship between crater-wear rate and average tool-chip interface temperature: 1) High-speed steel, 2) C-1 carbide, and 3) C-5 carbide (see Table 22.4). Note how rapidly crater-wear rate increases with an incremental increase in temperature. *Source*: After B. T Chao and K. J Trigger.

Cutting Tool Interface and Chip

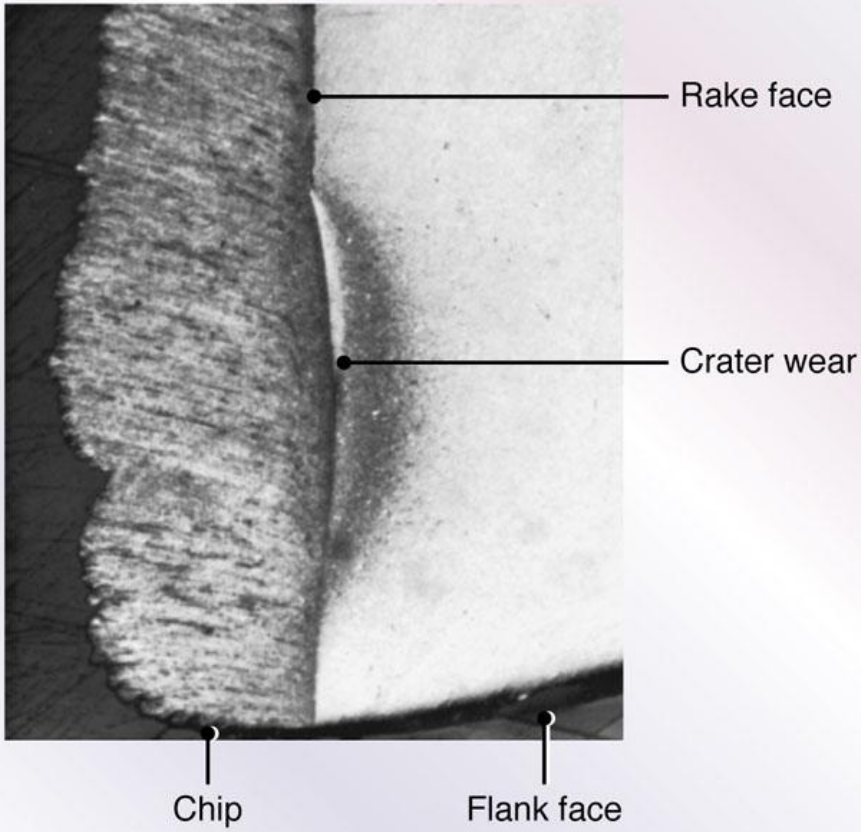

Figure 21.20 Interface of a cutting tool (right) and chip (left) in machining plain-carbon steel. The discoloration of the tool indicates the presence of high temperatures. Compare this figure with the temperature profiles shown in Fig. 21.12. *Source*: Courtesy of P. K. Wright.

Machined Surfaces Produced on Steel

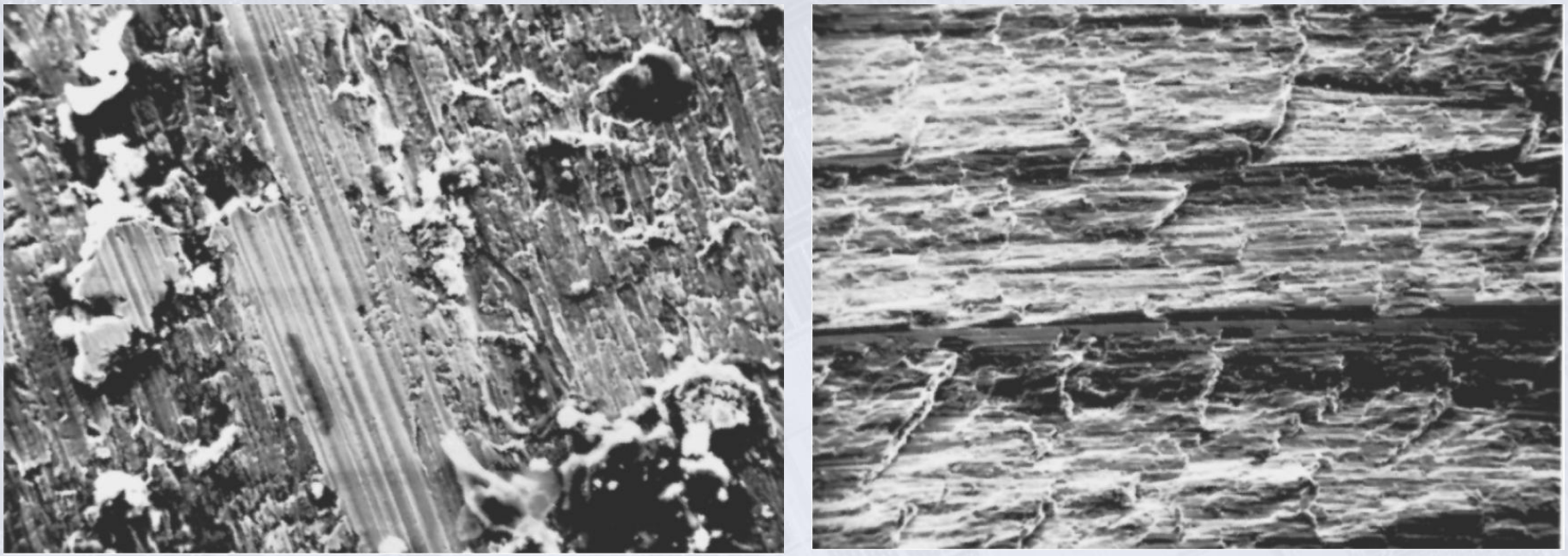

(a) **(b)**

Figure 21.21 Machined surfaces produced on steel (highly magnified), as observed with a scanning electron microscope: (a) turned surface and (b) surface produced by shaping. *Source*: Courtesy of J. T. Black and S. Ramalingam.

Dull Tool in Orthogonal Machining

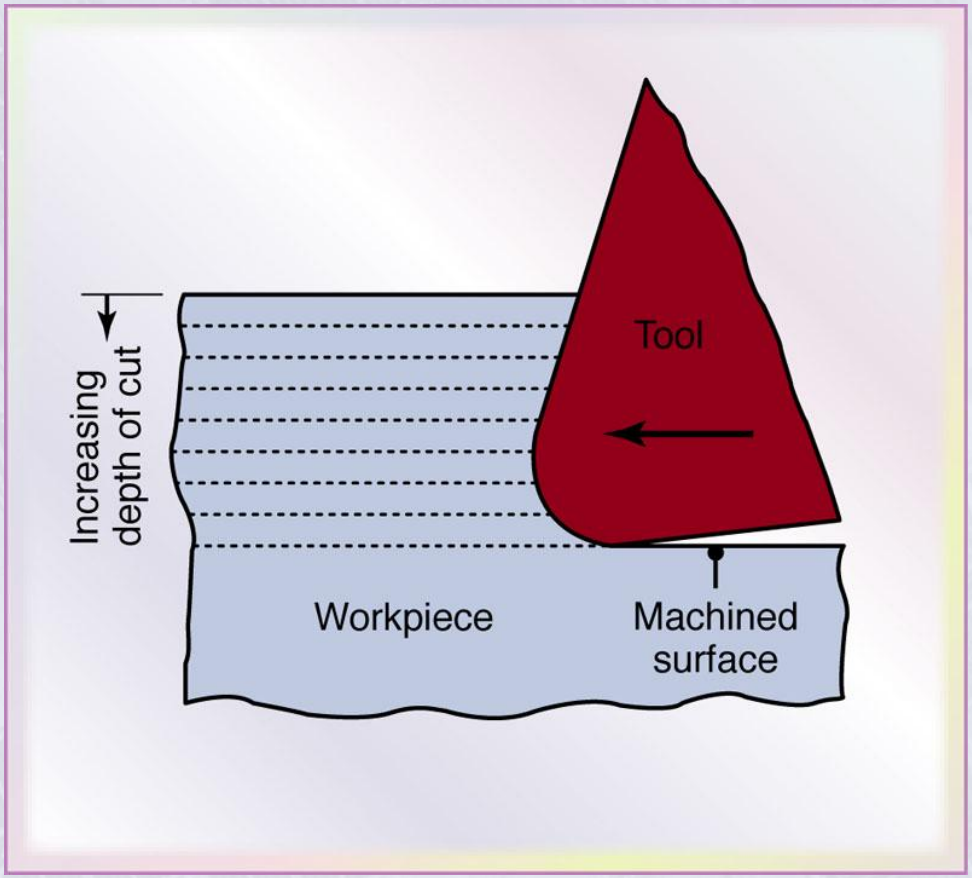

Figure 21.22 Schematic illustration of a dull tool with respect to the depth of cut in orthogonal machining (exaggerated). Note that the tool has a positive rake angle, but as the depth of cut decreases, the rake angle effectively can become negative. The tool then simply rides over the workpiece (without cutting) and burnishes its surface; this action raises the workpiece temperature and causes surface residual stresses.

Feed Marks on a Turned Surface

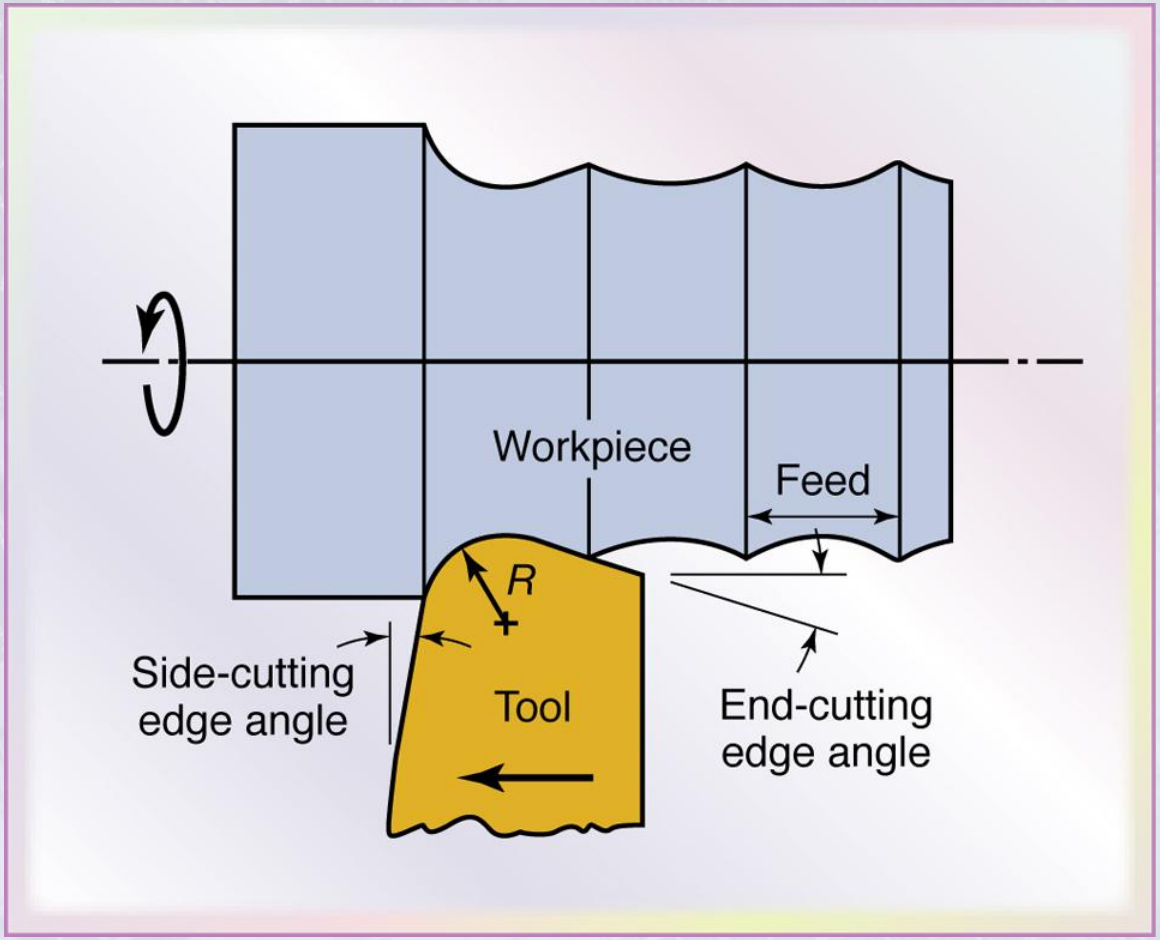

Figure 21.23 Schematic illustration of feed marks on a surface being turned (exaggerated).

Surface roughness:

$$R_a \approx \frac{f^2}{8R}$$

where

f = feed

R = tool-nose radi